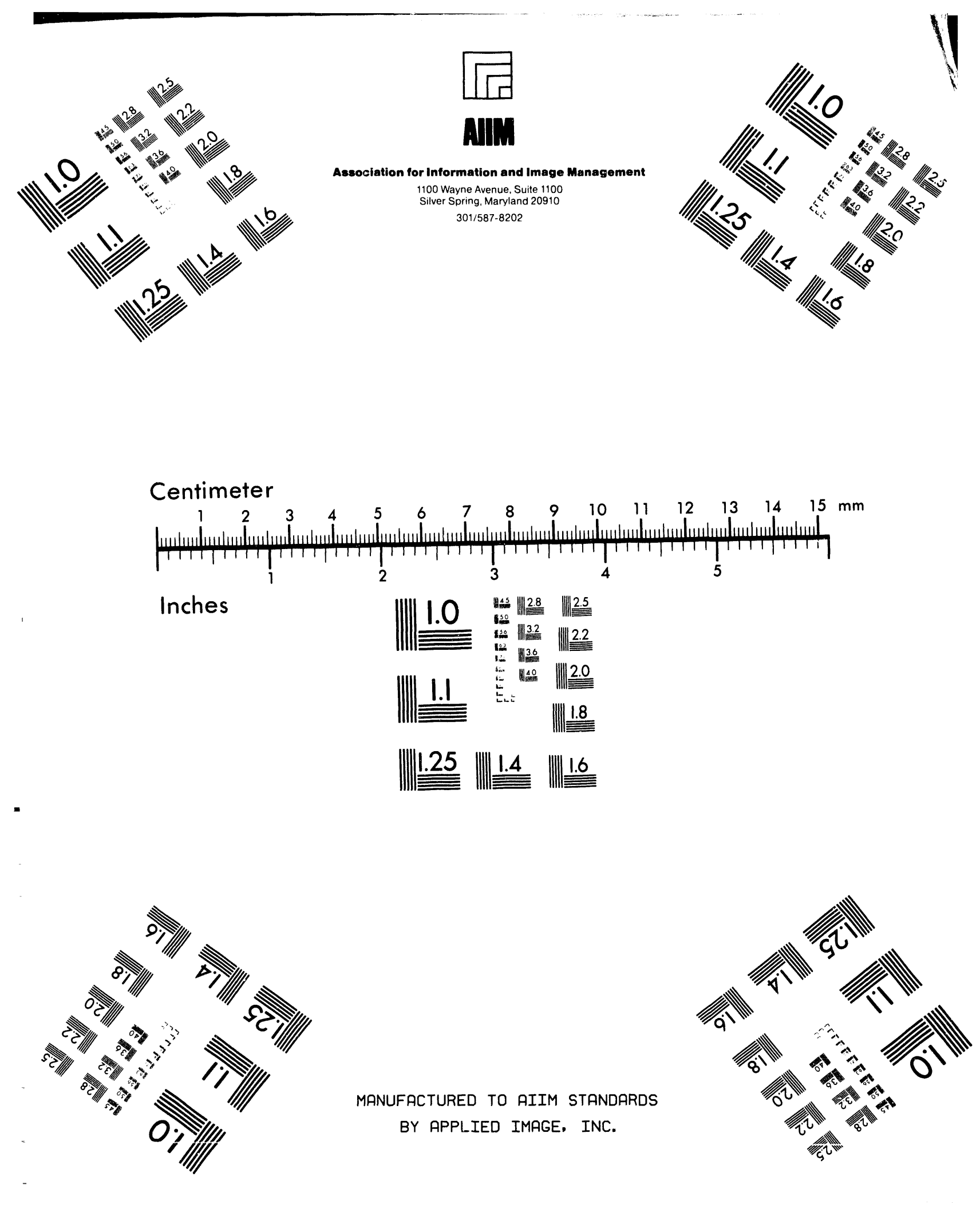
AIIM
Association for Information and Image Management
1100 Wayne Avenue, Suite 1100
Silver Spring, Maryland 20910
301/587-8202
Centimeter
Inches
MANUFACTURED TO AIIM STANDARDS
BY APPLIED IMAGE, INC.

1 of 1

DOE/PC/91296-6
Quarter report #6, 1/1/93-3/31/93
Advanced NMR-Based Techniques for Pore Structure Analysis of Coal

DE-FG22-91PC91296

Douglas M. Smith
UNM/NSF Center for Micro-Engineered Ceramics
University of New Mexico
Albuquerque, NM 87131
(505) 277-2861

Background

One of the main problems in coal utilization is the inability to properly characterize its complex pore structure. Coals typically have micro/ultra-micro pores but they also exhibit meso and macroporosity. Conventional pore size techniques (adsorption/condensation, mercury porosimetry) are limited because of this broad pore size range, microporosity, reactive nature of coal, samples must be completely dried, and network/percolation effects. Small angle scattering is limited because it probes both open and closed pores. Although one would not expect any single technique to provide a satisfactory description of a coal's structure, it is apparent that better techniques are necessary. Small angle scattering could be improved by combining scattering and adsorption measurements. Also, the measurement of NMR parameters of various gas phase and adsorbed phase NMR active probes can provide pore structure information. We will investigate the dependence of the common NMR parameters such as chemical shifts and relaxation times of several different nuclei and compounds on the pore structure of model microporous solids, carbons, and coals. In particular, we will study the interaction between several small molecules (^{129}Xe, ^{3}He, $^{2}H_2$, $^{14}N_2$, $^{14}NH_3$, $^{15}N_2$, $^{13}CH_4$, $^{13}CO_2$) and the pore surfaces in coals. The project combines expertise at the UNM (pore structure, NMR), Los Alamos National Laboratory (NMR), and Air Products (porous materials).

Work completed during the last quarter

Our current work may be divided into three areas: small-angle X-ray scattering (SAXS), adsorption, and NMR.

1. SAXS.

Previously, we studied scattering from samples of the porous glass, CPG 75, as a function of vapor loading. In this quarter, we studied samples of different porous materials, as well as particles, liquid loaded with different solvents with a wide range of electron density (η) compared to the porous substrates. The purpose of this portion of the work was to demonstrate that we were indeed contrast-matching the solid matrix with dibromomethane since the CPG 75 sample still exhibited some scattering when the pores were fully loaded with fluid. The samples we have

studied this quarter were CPG 350, similar to CPG 75 but with a nominal pore diameter of 35 nm, silica gel from Alltech, fumed silica, and a microporous carbon.

From the stack plot of liquid loaded samples of CPG 350 (fig. 1) we find that the degree of contrast matching does indeed vary with the solvent electron density. This is a apparent in both the disappearance of the peak at q= 0.01 $Å^{-1}$ and the decrease in intensity. The peak at has been previously assigned to the CPG pores. The complete disappearance of the peak indicates very good contrast matching. As expected, we find that the sample liquid loaded with chloroform does not match well. The samples liquid loaded with dibromomethane, 1,2-dibromoethane and chlorodibromomethane show very good contrast match as there is no inflection point in the curves obtained from the SAXS data. From the literature, we find that the above three solvents are the closest in electron density to the porous substrate. The bromoform loaded sample has a larger electron density which is evident in the inflection at the position of the peak. This is a good example of how SAXS only is insensitive to the density of the scatterers but rather, only the density difference.

For carbon which has been liquid-loaded, we find that the curves (fig. 2) flatten out at high q values for all samples. Compared to the curve for the blank carbon, we find that this is an indication of good contrast match. The bromoform and dibromomethane loaded samples match pretty well. The chlorodibromomethane loaded sample shows a slight inflection indicating that it is not as a good match since this implies that the pore space is not filled with a solvent of the same electron density as that of the solid matrix. This is slightly different than the results for the CPG 350 samples. This is because the electron density of carbon is different from that of silica. We should note that the calculated electron density assumes the sample is SiO_2. In fact, these high surface area silicas will contain a substantial amount of hydroxyl groups on the surface which will lower the electron density. Therefore, the fluid which provides the best match depends on the exact nature of the porous solid. However, this effect is not a major problem since the intensity varies with the square of the density difference. From the above results, we observe that the carbon has a higher electron density than silica.

We conducted similar contrast matching studies on silica gel obtained from Alltech to confirm our results of CPG 350. We find a trend (fig. 3) similar to that of CPG 350. The chloroform loaded sample does not match indicating a difference in the electron density between the solid matrix and the solvent filling the pore space. The three solvents dibromomethane, 1,2-dibromoethane and chlorodibromomethane have the best contrast match. The bromoform loaded sample of silica shows a discontinuity in electron density. We then studied the scattering of L90, a fumed silica, liquid loaded with chloroform and the three solvents closest in electron density. The results shown in fig. 4 are similar to those obtained for silica gel and CPG 350.

2. ADSORPTION.

During the last quarter, results were reported on the adsorption of methane, carbon dioxide, and nitrogen on a series of microporous carbons supplied by our industrial partner, Air Products. Surface areas as determined by various methods were reported and differences in the adsorption of the three adsorbate gases were

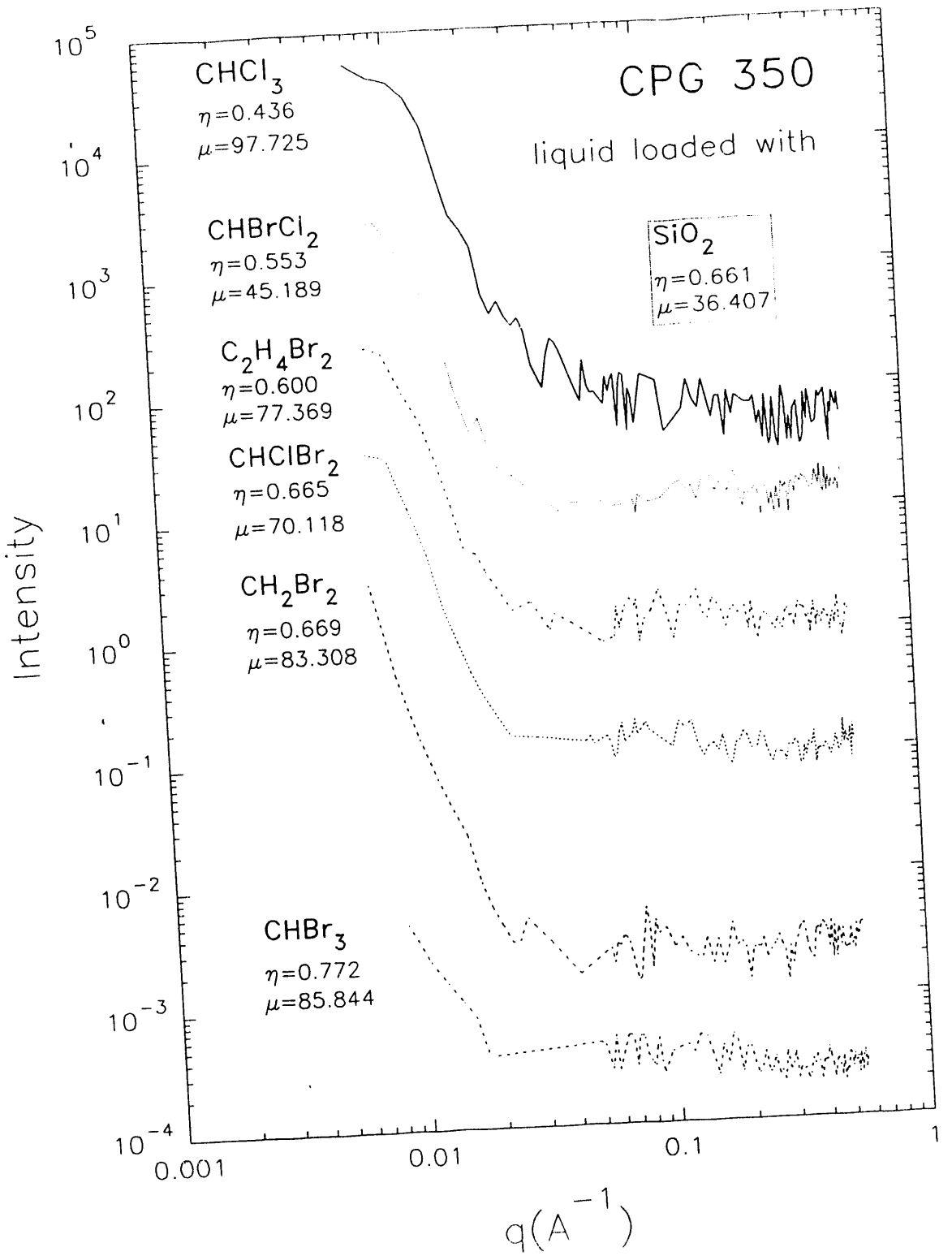

Figure 1 SAXS as a function of liquid loading fluid electron density for CPG 350.

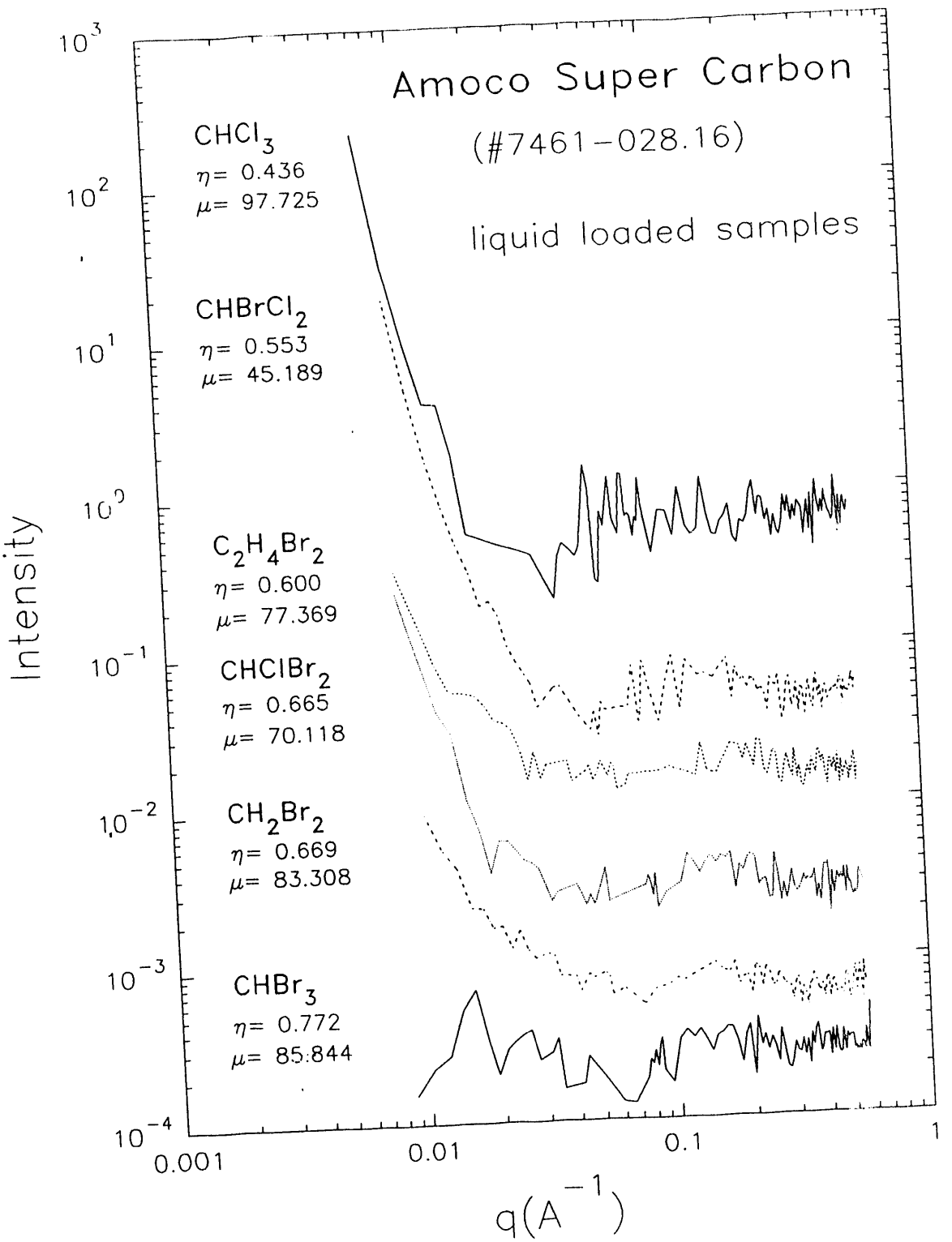

Figure 2 SAXS as a function of electron density for liquid saturated Amoco super carbon.

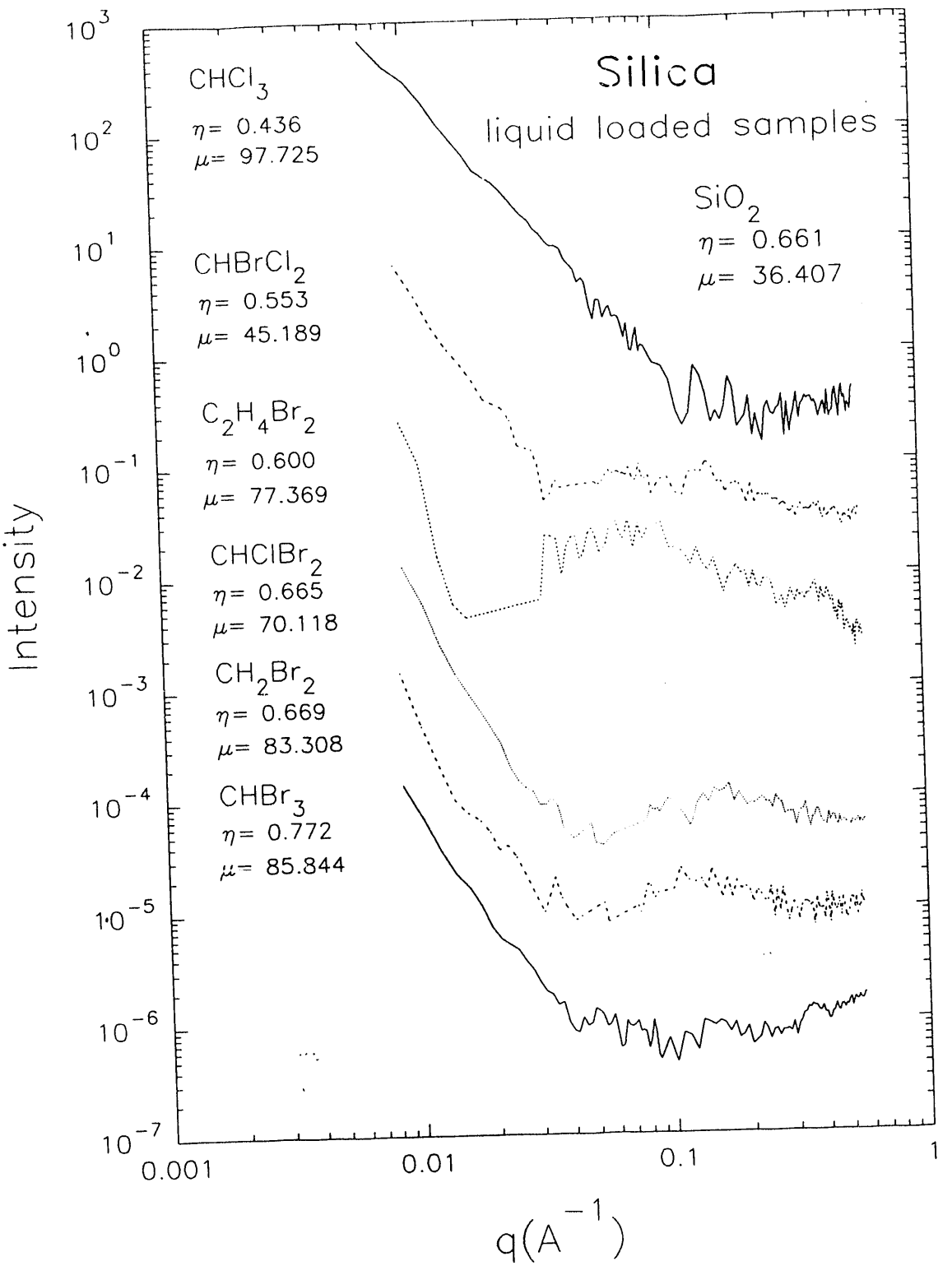

Figure 3 SAXS as a function of pore fluid electron density for Alltech silica gel.

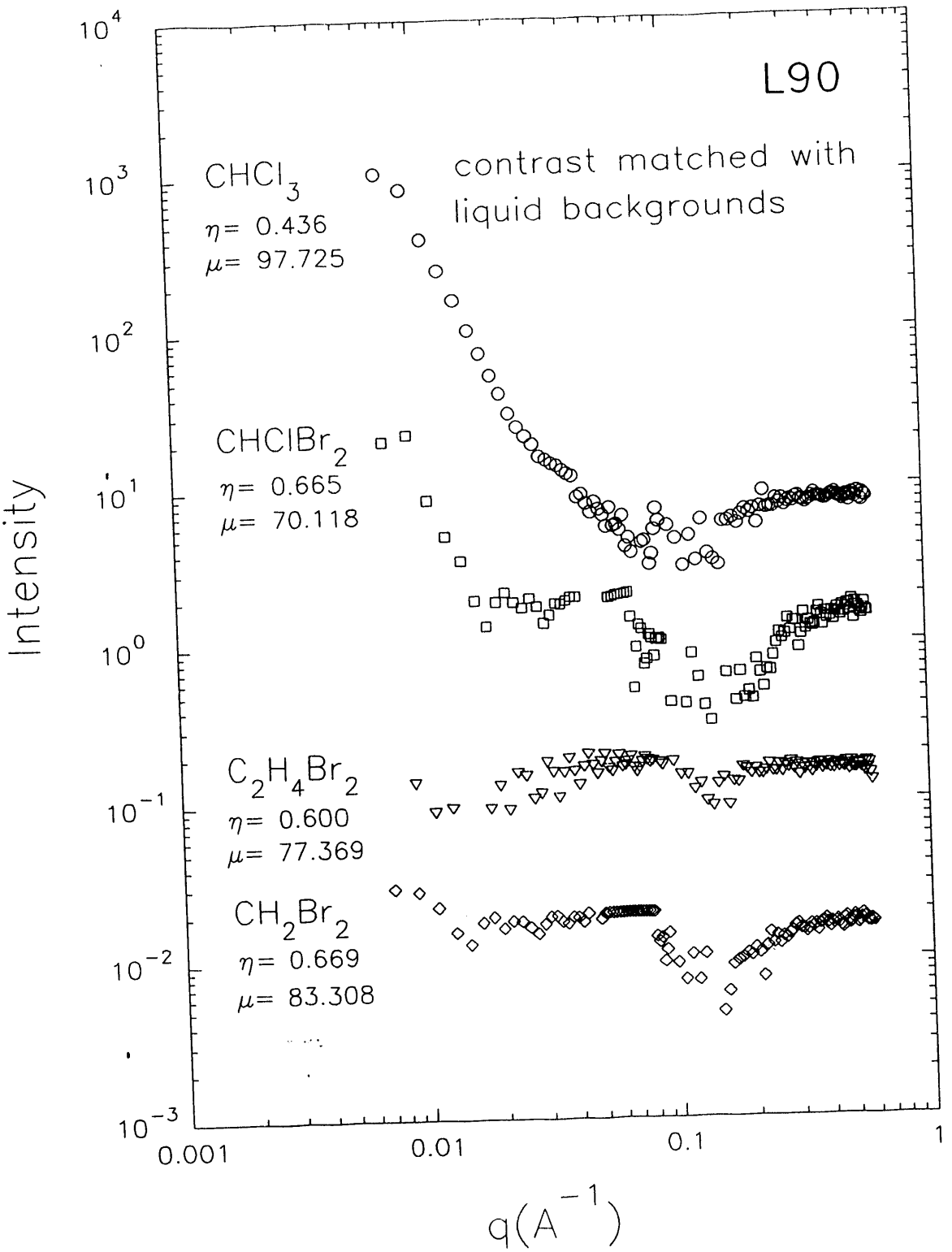

Figure 4 SAXS as a function of fluid electron density for L90 silica particles.

explained on the basis of differences between the gas molecules and the heterogeneity of the adsorbent itself.

At the beginning of this quarter it was decided to cross-check the high pressure methane isotherms. These isotherms were initially determined using a manually operated high pressure volumetric gas adsorption system. Early in this quarter, an automated high-pressure volumetric adsorption unit, capable of measuring adsorption isotherms up to 25,000 Torr (484 psia) was procured from VTI Corporation, Hialeah, Florida. This unit, the HPA 100, is fully computer controlled and the CH_4 isotherms were remeasured using this system.

The previous CH_4 isotherms continued to slant upwards with a positive slope at high pressures, instead of flattening out and reaching a plateau as would be expected for a microporous solid. Earlier it was assumed that this was due to continued pore filling at higher pressures. However, it appears that inaccuracies in the initial manual measurement could have contributed to this continued positive slope. The remeasured CH_4 isotherms are somewhat flatter (see Fig. 5), the isotherms flatten out at higher pressures indicating that saturation uptake has been reached. The Dubinin-Astakhov (DA) plots have been determined for the new high pressure data combined with the previous low-pressure data and these are reproduced in Fig. 6. Recalculation of the DA surface areas and DA exponents gives the values in Table 1. The new values of DA surface area are lower than those previously reported. The DA exponents, which, as mentioned earlier, are a measure of the energetic heterogeneity of the adsorbent surface, indicate a narrower distribution than derived from the previous CH_4 data. Some of the anomalies in the previously reported results are thus accounted for (please refer to previous reports).

Also during this quarter, helium pycnometry was carried out on the same series of carbon samples in order to determine the skeletal densities of the samples. It is possible that in the narrowest pores, helium could be adsorbed which will contribute to errors in isotherm measurement as helium is used for determining the free space available to the adsorbate gas. The results are listed in Table 1. For two of the samples (7461-071.19 and 7461-058.57) the run was abandoned because equilibrium could not be attained, indicating narrow pore openings where restricted diffusion could be taking place. All the carbons gave reasonable values for skeletal density (as compared to 2.27 g/cm^3 for graphite).

3. NMR Techniques.

During the quarter, a series of NMR experiments were conducted using ^{129}Xe and $^{15}N_2$ as a function of temperature. The main thrust of this work was two-fold. First, imogolite tubular aluminosilicates were studied as a function of outgassing temperature. We were interested in seeing if the two distinct pore types associated with the inner diameters of the tubes (0.8 nm) and the pores associated with the region between three tubes which are in a close-packed array (~0.3 nm). The second part of our NMR effort is directed at understanding the change in freezing point of fluids in microporous solids as a means of determining pore size. Freezing point depression has been used to determine pore size for solids by using

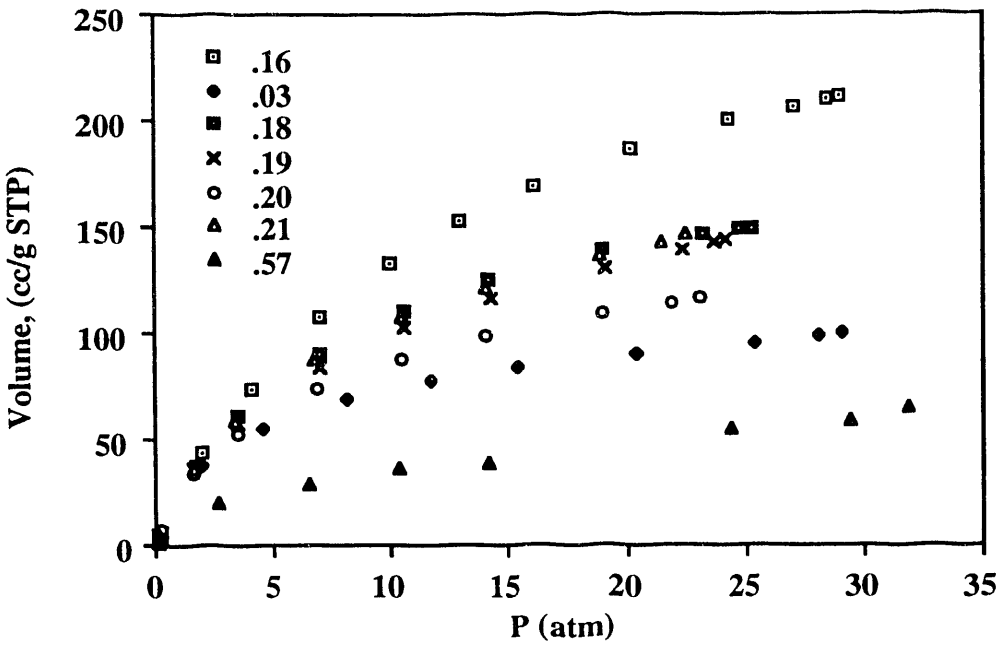

Figure 5 New high pressure methane (295 K) isotherms for carbons series

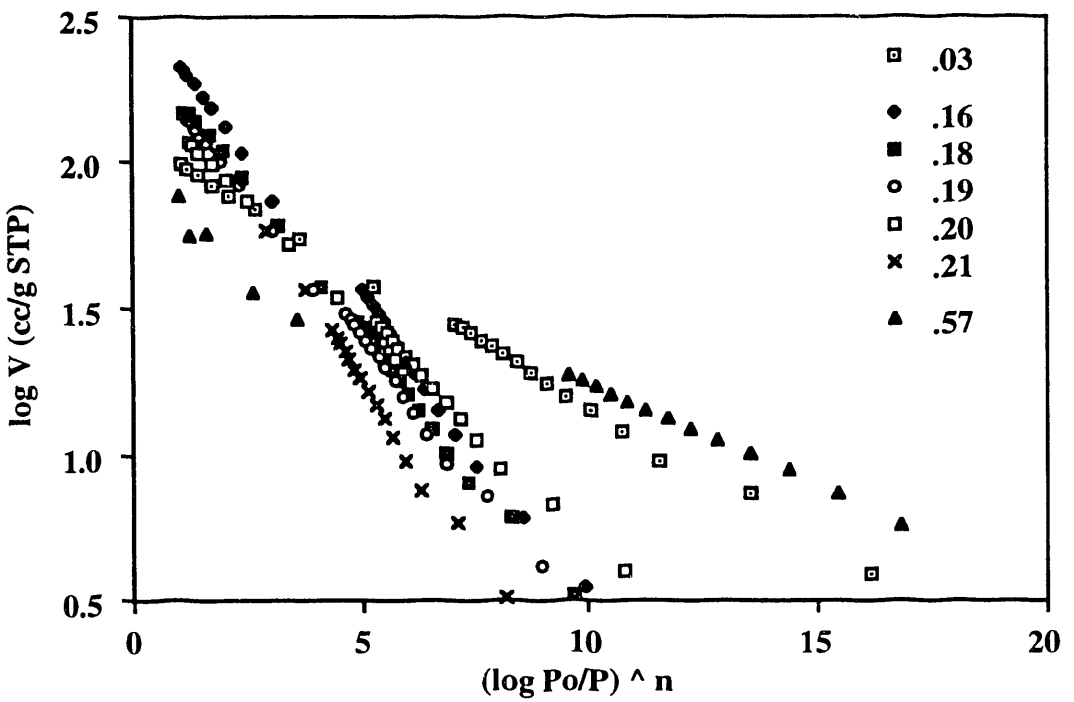

Figure 6 New methane (295 K) DA plots for carbons series.

TABLE 1 Comparison of results obtained from methane (295 K) on VTI HPA 100 system with previous results (manual system)

Sample ID, 7461-	DA surface area, CH_4, m^2/g, previous	DA surface area, CH_4, m^2/g, current	DA exponent CH_4, previous	DA exponent CH_4, current	DA surface area, CO_2, m^2/g	DA exponent CO_2	Skeletal density, g/cm^3
071.03	599	455	1.9	2.13	809	1.81	1.95
028.16	1320	1142	1.65	1.75	2693	1.24	2.41
071.18	1103	871	1.56	1.73	1663	1.35	2.35
071.19	961	822	1.59	1.68	1322	1.45	NA
071.20	669	632	1.78	1.82	1053	1.68	2.24
071.21	1307	966	1.45	1.61	1577	1.39	2.33
058.57	248	242	2.62	2.46	507	2.01	NA

DSC to determine the distribution of freezing point. In this work, our results indicate that the freezing point (in a NMR sense) decreases with pore size until pores in the microporous size range (radius <1 nm) are probed. For ultramicropores, the motion of the probe molecules is restricted such that freezing actually occurs at elevated temperatures as compared to freezing in mesoporosity (but the freezing point is still less than the bulk freezing point of the fluid). We are currently using a series of different tubular aluminosilicates to study this effect.

Work planned for next quarter

Our goals for the next quarter include:

1. Measure adsorption isotherm of contrast-matched adsorbates such as dibromomethane on CPG-75, CPG-350, Cabot L-90, and Alltech silica gel. Relate the change in scattering curves versus the thickness of adsorbed film to pore structure parameters such as pore surface roughness, pore geometry, and pore size distribution.

2. Continue ^{129}Xe, $^{14}N_2$, $^{14}CH_4$ and $^{15}N_2$ NMR experiments of fluids adsorbed in porous solids. This will include using a series of specially prepared silica xerogels which will allow us to vary the pore size over a wide range (1-50 nm) with no change in surface chemistry.

DATE
FILMED
9/9/93

END